



**HAL**  
open science

## Probing the Importance of Host Symmetry on Carbohydrate Recognition

Anne-Doriane Manick, Chunyang Li, Elise Antonetti, Muriel Albalat, Yoann Cotelle, Paola Nava, Jean-Pierre Dutasta, Bastien A Chatelet, Alexandre Martinez

► **To cite this version:**

Anne-Doriane Manick, Chunyang Li, Elise Antonetti, Muriel Albalat, Yoann Cotelle, et al.. Probing the Importance of Host Symmetry on Carbohydrate Recognition. *Chemistry - A European Journal*, 2023, pp.e202203212. 10.1002/chem.202203212 . hal-03961776

**HAL Id: hal-03961776**

**<https://hal.science/hal-03961776>**

Submitted on 29 Jan 2023

**HAL** is a multi-disciplinary open access archive for the deposit and dissemination of scientific research documents, whether they are published or not. The documents may come from teaching and research institutions in France or abroad, or from public or private research centers.

L'archive ouverte pluridisciplinaire **HAL**, est destinée au dépôt et à la diffusion de documents scientifiques de niveau recherche, publiés ou non, émanant des établissements d'enseignement et de recherche français ou étrangers, des laboratoires publics ou privés.



Distributed under a Creative Commons Attribution - NonCommercial - NoDerivatives 4.0  
International License

# Probing the Importance of Host Symmetry on Carbohydrate Recognition

Anne-Doriane Manick<sup>+, [a]</sup> Chunyang Li<sup>+, [b]</sup> Elise Antonetti,<sup>[a]</sup> Muriel Albalat,<sup>[a]</sup> Yoann Cotelle,<sup>[a]</sup> Paola Nava,<sup>[a]</sup> Jean-Pierre Dutasta,<sup>[c]</sup> Bastien Chatelet,<sup>\*, [a]</sup> and Alexandre Martinez<sup>\*, [a]</sup>

**Abstract:** The design of molecular cages with low symmetry could allow for more specific tuning of their properties and better mimic the unsymmetrical and complex environment of protein pockets. However, the added value of lowering symmetry of molecular receptors has been rarely demonstrated. Herein,  $C_3$ - and  $C_1$ -symmetrical cages, presenting the same recognition sites, have been synthesized and investigated as hosts for carbohydrate recognition. Structurally related derivatives of glucose, galactose and mannose were

found to have greater affinity to the receptor with the lowest symmetry than to their  $C_3$ -symmetrical analogue. According to the host cavity modelling, the  $C_1$  symmetry receptor exhibits a wider opening than its  $C_3$ -symmetrical counterpart, providing easier access and thus promoting guest proximity to binding sites. Moreover, our results show the high stereo- and substrate selectivity of the  $C_1$  symmetry cage with respect to its  $C_3$  counterpart in the recognition of sugars.

## Introduction

In recent years, artificial molecular containers have attracted a wide attention.<sup>[1,2]</sup> Their well-defined cavity mimics the binding pockets of the proteins, giving rise to new receptors,<sup>[3-8]</sup> or supramolecular catalysts.<sup>[9-17]</sup> These bio-inspired cages differ from natural ones by various features, one of the most striking being the level of symmetry.<sup>[18-24]</sup> Indeed, cavities in proteins present a low level of symmetry, affording complex unsymmetrical environment around recognition or catalytic sites, whereas synthetic cage compounds are of high symmetry probably because of their easier and more direct synthesis and more convenient analysis of the resulting systems. Artificial cages with lower symmetry aroused recently a growing interest as they may allow to tune more specifically the inner space of the cavity, leading to a better control of its properties.<sup>[18-24]</sup> Indeed, biomolecules are scarcely highly-symmetrical com-

pounds, thus lowering the symmetry of artificial receptors appears as a promising strategy to bind such substrates.<sup>[19]</sup> However, there is still a very limited number of cage compounds with low symmetry that present improved properties compared to their highly symmetrical parents.<sup>[18,25]</sup> Herein we report on the synthesis of two covalent hemicryptophane cages that display the same lower and upper units as well as the same linkers, and only differ by their symmetry. Their recognition properties towards carbohydrates were investigated and the  $C_1$ -symmetrical host reveals much better affinities for this class of guests than its  $C_3$ -symmetrical counterpart. The same trend was observed in favor of the  $C_1$ -symmetrical cage when considering stereo- and substrate selectivity, underlining the importance of the host symmetry in carbohydrates recognition.

## Results and Discussion

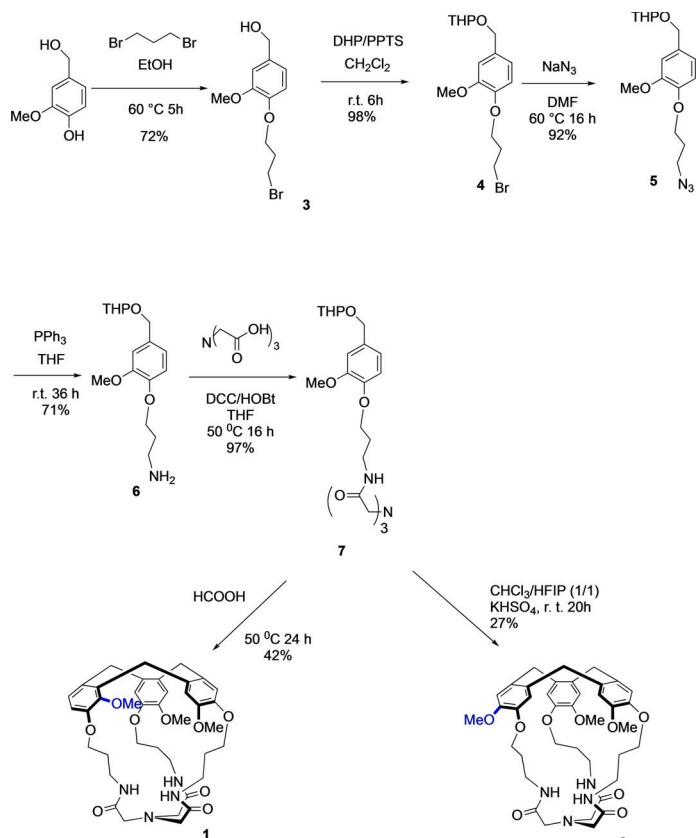
We have previously described the synthesis of the enantiopure hemicryptophane cage  $C_1$ -1 combining a cyclotrimeratrylene (CTV) moiety with an amino-trisamide unit exhibiting a  $C_1$  symmetry (Scheme 1).<sup>[26]</sup> This low symmetry was due to an unexpected arrangement of the substituents of the CTV cap, although a conventional cyclisation in formic acid was used to synthesize this unit. In order to compare the binding properties of the  $C_1$  symmetrical receptor  $C_1$ -1 with its  $C_3$  symmetrical parent  $C_3$ -2, attempts were performed to obtain the cage with higher symmetry (Scheme 1). The use of scandium triflate, in the presence of the cyclisation precursor **7**, only provides polymers. As conventional cyclisation procedure (HCOOH) gives the unusual  $C_1$  CTV moiety, we hypothesized that an unconventional procedure for the synthesis of the CTV cap could lead to the expected  $C_3$  symmetry compound. We have recently reported that the use of the bisulfate salt/HFIP (Hexafluoroiso-

[a] Dr. A.-D. Manick,<sup>+</sup> E. Antonetti, Dr. M. Albalat, Y. Cotelle, P. Nava, Dr. B. Chatelet, Prof. A. Martinez  
Aix Marseille Université  
Centrale Marseille, CNRS, iSm2 UMR 7313,  
13397 Marseille (France)  
E-mail: alexandre.martinez@centrale-marseille.fr  
bastien.chatelet@centrale-marseille.fr

[b] Dr. C. Li<sup>+</sup>  
School of Materials Science and Engineering, Sichuan University of Science & Engineering, Zigong, 643000, China  
and  
Material Corrosion and Protection Key Laboratory of Sichuan Province, Sichuan University of Science & Engineering, Zigong, 643000, China

[c] Dr. J.-P. Dutasta  
ENSL, CNRS, Laboratoire de Chimie UMR 5182  
46 allée d'Italie, 69364 Lyon (France)

[<sup>+</sup>] These two authors contributed equally to this manuscript.



**Scheme 1.** Synthesis of  $C_3$ -symmetrical cage  $C_3$ -2 and the previously obtained  $C_1$ -symmetrical cage  $C_1$ -1.<sup>26</sup>

propanol) combination strongly affects the regioselectivity of the ring closure Friedel-Crafts reaction leading to CTV, allowing for an easier access to the syn-cryptophane stereoisomers. This prompted us to examine if the use of HFIP as co-solvent could also promote the synthesis of hemicryptophanes and change the selectivity of this cyclisation reaction.<sup>[27]</sup>

The precursor **7** was synthesized in five steps following our previously reported procedure (Scheme 1): 1,3-dibromopropane reacted with vanillyl alcohol in ethanol, leading to compound **3** that was then protected with a THP group to give **4** (71% for the two steps). Then, addition of sodium azide to **4** in DMF solution afforded **5** with 92% yield. The azide function was then reduced using triphenylphosphine, providing **6** in 71% yield. The subsequent reaction of nitrilotriacetic acid with compound **6** using DCC/HOBt as coupling agent gave the expected precursor of cyclisation **7**. The reaction of formation of the CTV unit was performed in the presence of  $\text{KHSO}_4$  (0.9 equiv.) using a mixture of  $\text{CHCl}_3$ /HFIP (1/1, v/v) as solvent and stirred overnight at room temperature. The  $^1\text{H}$  NMR spectrum of the crude reaction mixture showed signals corresponding to the  $C_1$ -symmetrical cage  $C_1$ -1 and new signals that were attributed to the  $C_3$ -symmetrical hemicryptophane  $C_3$ -2 respectively in the 18:82 ratio (Figure 1). The use of chiral HPLC allowed for the resolution of the racemic mixture  $C_3$ - $(\pm)$ -2, providing the two enantiomers of  $C_3$ -2 with high enantiomeric excess ( $ee > 99.5\%$ , Figures S14 and S16). The chromatogram confirmed the ratio of cage  $C_1$  to cage  $C_3$ -2 measured by  $^1\text{H}$  NMR (Figure 2a). The

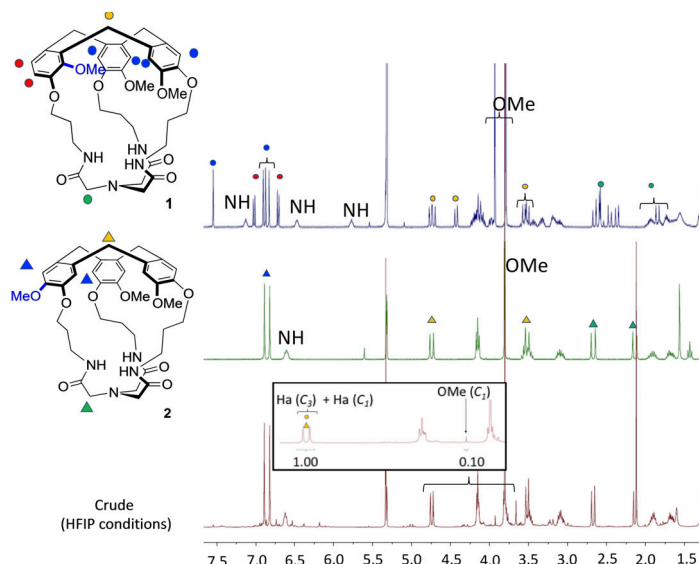


**Figure 1.**  $^1\text{H}$  NMR spectra (300 MHz,  $\text{CD}_2\text{Cl}_2$ ) of  $C_1$ -1,  $C_3$ -2 and the crude reaction mixture using the HFIP procedure.

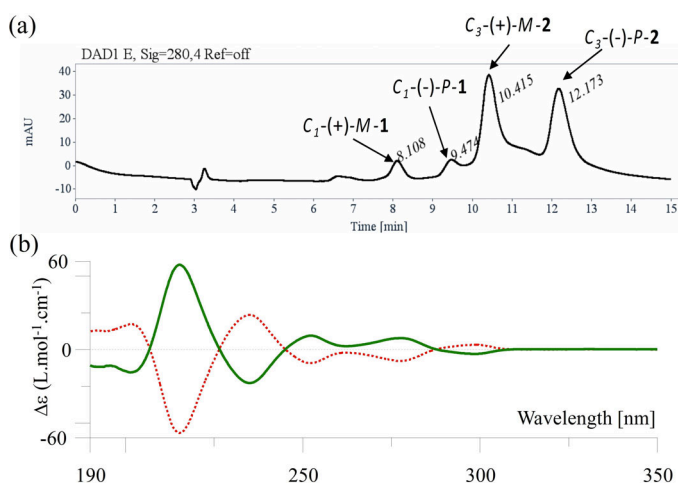


**Figure 2.** (a) HPLC chromatogram of the mixture obtained after cyclisation in HFIP ( $(S,S)$ -Whelk-O1; eluent: hexane/ethanol +  $\text{Et}_3\text{N}$  0.5%/dichloromethane (30/40/30)); (b) ECD spectra of  $C_3$ - $(+)$ -M-2 (green solid line) and  $C_3$ - $(-)$ -P-2 (red dotted line) in acetonitrile ( $C = 0.25 \text{ mmol}\cdot\text{L}^{-1}$ ).

electronic circular dichroism (ECD) spectra of the two enantiomers of  $C_3$ -2 were then recorded to assign their absolute configuration (Figure 2b). Indeed, the sign of the exciton pattern centers on the  $^1L_a$  transition ( $\sim 240 \text{ nm}$ ) can be compared to a CTV of known absolute configuration as this band weakly depends on the substituents linked to the CTV moiety.<sup>[28]</sup> Thus, the  $C_3$ - $(+)$ -M-2 and  $C_3$ - $(-)$ -P-2 configurations were assigned to the first and second eluted enantiomers, respectively.

Although modest, the yield is in the same range of values as those usually obtained in the synthesis of hemicryptophane cages.<sup>[7b]</sup> Indeed, this cyclization step involved the simultaneous formation of three macrocycles and side reactions, leading to oligomers or polymers, are difficult to avoid.

The NMR analysis of pure cage  $C_3$ -2 supports the  $C_3$  symmetry of this compound; the characteristic signals of the  $C_3$  symmetrical CTV unit appear in the  $^1\text{H}$  NMR spectrum: a singlet for the OMe groups at 3.81 ppm, two doublets for the diastereotopic protons of the  $\text{CH}_2$  groups at 4.75 and 3.52 ppm with the characteristic coupling constant of 13.7 Hz, and two singlets for the aromatic protons (6.88 and 6.82 ppm). The signals corresponding to NH and  $\text{CH}_2$  of the trisamide lower part can be observed at 6.52 and 2.66 and 2.09 ppm respectively and finally those of the diastereotopic methylene appears as a complex pattern between 3.58 and 1.61 ppm. This result confirms that the use of HFIP allows for (i) the formation of the CTV unit leading to hemicryptophane cage, (ii) a change in the selectivity of this cyclisation step as previously observed for cryptophane cages.<sup>[27]</sup> This highlights the potential of this new method for the synthesis of host molecules based on the CTV moiety.

With these two cages  $C_1$ -1 and  $C_3$ -2 in hand, which differ only in their level of symmetry, we decided to compare their recognition properties using carbohydrates as guests. As the complexation of carbohydrates is a key point in numerous biological processes such as infection by pathogens<sup>[29]</sup> or tumor metastases,<sup>[30]</sup> synthetic receptors<sup>[31]</sup> including, for instance, platforms,<sup>[32]</sup> Macrocyles,<sup>[33]</sup> covalent or self-assembled cages<sup>[34,35]</sup> and foldamers,<sup>[36]</sup> have been developed to create new tools for therapies or diagnoses. Most of these receptors display a high level of symmetry, and low-symmetry carbohydrate hosts have been scarcely described. For instance, Davis et al. have reported synthetic lectins presenting different 'floor' and 'roof' for the selective recognition of glucose.<sup>[25]</sup>

In this context, the direct comparison of the binding properties of carbohydrates by two cages bearing the same complexation units but differing only by their level of symmetry could shed light on the importance of host symmetry for the recognition of chiral guests. Moreover, the recognition of carbohydrates makes it possible to evaluate the influence of lowering the symmetry both on the value of the association constant and on the stereo- and substrate selectivity of the recognition process. Indeed, most carbohydrates differ in the stereochemistry of only one of the five stereogenic centers, making substrate selective complexation hard to achieve. To this end, NMR titrations experiments were performed with *n*-octyl glucose, galactose, and mannose derivatives as guest molecules (Figures 3 and S19, Table 1). A preliminary control experiment was carried out using *n*-octane as guest and no complexation was observed, ruling out any specific interaction of the cages with the *n*-octyl chain of the carbohydrate derivatives (Figure S69). It can be noticed that, during the titration experiments with the carbohydrate guests, the signals corresponding to the NH protons of the hosts amide functions are downfield shifted supporting  $\text{NH}\cdots\text{O}$  hydrogen-bonding with the alcohol functions of the guests (Figure S24). Two different sets of  $^1\text{H}$  NMR signals ( $\text{CH}_2\text{-NH-}$  and  $-\text{CH}_2\text{-C(O)NH-}$ ) were followed to obtain the titration curves which were fitted using Bindfit software, providing binding constants shown in Figure 3 and Table 1.<sup>[37]</sup> It appears that the  $C_1$  symmetrical cage  $C_1$ -1 exhibits much higher affinities for carbohydrates than its  $C_3$

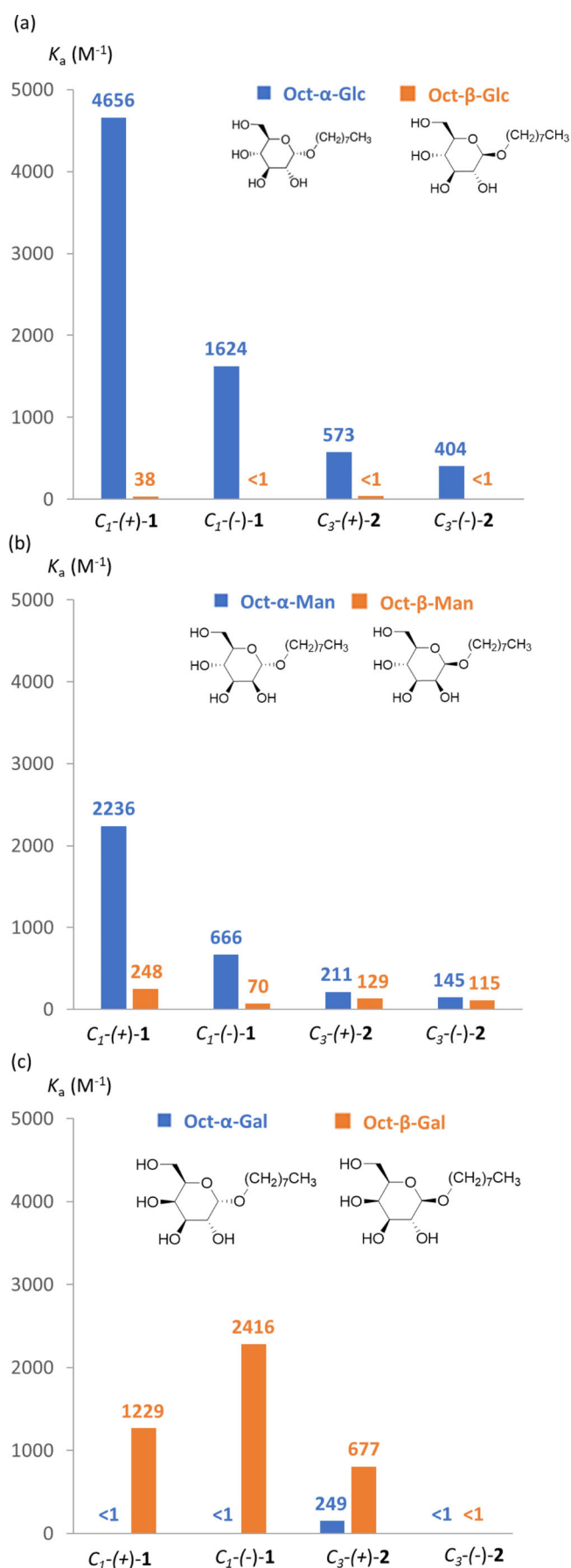


**Figure 3.** Association constants using cages  $C_1$ -1 and  $C_3$ -2 as hosts and glucose, mannose, or galactose as guests.  $K_a$  was determined by fitting  $^1\text{H}$  NMR titration curves ( $\text{CD}_2\text{Cl}_2$ , 500 MHz, 300 K) with Bindfit program.<sup>37</sup> More details on the calculations results can be found in Table S1; estimated error 10%.

**Table 1.** Affinity constants,  $K_a$  ( $L \cdot mol^{-1}$ ) for the association between the hosts and the guests at 300 K in  $CD_2Cl_2$ . The results reported in this table have been obtained from the fit of the titration curves with Bindfit program.

Guest Host	$K_a$ [ $M^{-1}$ ] <sup>[a]</sup>					
	Octyl- $\alpha$ -Glc	Octyl- $\beta$ -Glc	Octyl- $\alpha$ -Man	Octyl- $\beta$ -Man	Octyl- $\alpha$ -Galac	Octyl- $\beta$ -Galac
$C_1$ -(+)-1	4656	38	2236	248	< 1	1229
$C_1$ -(-)-1	1624	< 1	666	70	< 1	2416
$C_3$ -(+)-2	573	< 1	211	129	249	677
$C_3$ -(-)-2	404	< 1	145	115	< 1	< 1

[a]  $K_a$  is an average of two  $K_a$  values obtained by modelling two different titration curves, following two different  $^1H$  NMR signals ( $\underline{CH_2-NH-}$  and  $\underline{-CH_2-C(O)NH-}$ ).

symmetrical analogue  $C_3$ -2. For instance, the association constant is ten times higher with  $C_1$ -(+)-1 than with  $C_3$ -(+)-2 when the Oct- $\alpha$ -Glc glucose derivative is used as the guest ( $K_a = 4656 M^{-1}$  and  $573 M^{-1}$  respectively). With the Oct- $\alpha$ -Man mannose derivative, the similar trend is observed with a  $K_a$  of  $2236 M^{-1}$  for  $C_1$ -(+)-1 compared to  $211 M^{-1}$  determined with the host  $C_3$ -(+)-2. Although these two cages display exactly the same recognition units, they differ greatly in their complexation properties with respect to carbohydrates, the presence of a larger opening in the  $C_1$  symmetrical cage  $C_1$ -1 could account for this experimental result. Indeed, hosts  $C_1$ -1 and  $C_3$ -2 display similar cavity sizes ( $146.7$  and  $144.4 \text{ \AA}^3$ , respectively) but shapes strongly differ (Figure 4).<sup>[38]</sup> Whereas the access to the inner space of cage  $C_3$ -2 is strongly limited by three narrow windows, hemicryptophane  $C_1$ -1 presents a much larger window, allowing a better proximity with the recognition sites.

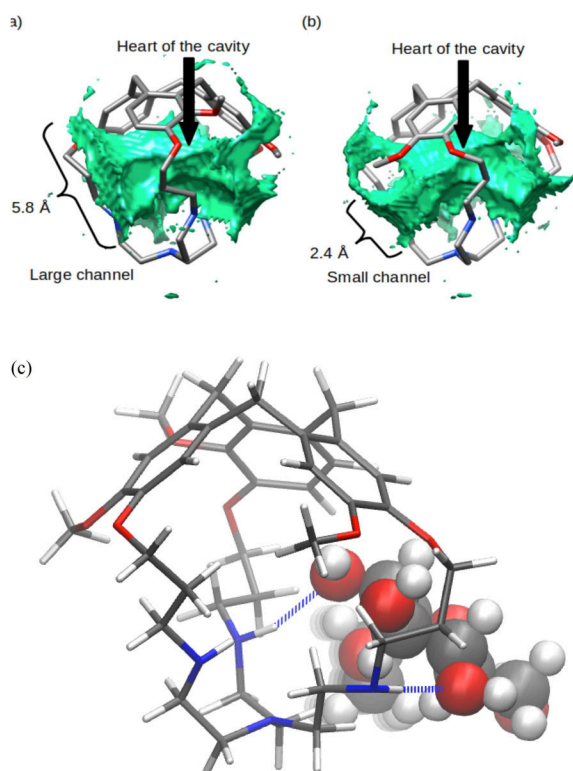


**Figure 4.** Views of the shape of the cavities of (a)  $C_1$ -1 and (b)  $C_3$ -2, and their calculated volumes (in green). Hydrogen atoms are omitted for clarity. (c) Optimized DFT structure of the Oct- $\alpha$ -Glc@ $C_1$ -(+)-1 complex.

NOESY experiments were performed on an equimolar solution of Oct- $\alpha$ -Glc and  $C_1$ -(+)-1; however, signals overlap precluded to assign unambiguously the intermolecular contacts. DFT calculations of the Oct- $\alpha$ -Glc@ $C_1$ -(+)-1 complex were then performed (Figures 4c and S74). The structure of the complex is more stable than the free guest and host by  $9.75 \text{ kJ/mol}$  and shows a partial encapsulation of the guest near the largest opening of the host cavity, a situation already observed with hemicryptophane complexes.<sup>[39]</sup> Two hydrogen bonds between the NH of the cage and the OH of the guest can be evidenced, in agreement with the downfield shifts of the amide protons observed during the  $^1H$  NMR titration experiments. Moreover, the distance between the two OH groups of the guest involved in the H-bonding is  $4.8 \text{ \AA}$ , smaller than the size of the window of the  $C_1$  symmetrical cage  $C_1$ -1 ( $5.8 \text{ \AA}$ ) but larger than that of the  $C_3$  symmetrical cage  $C_3$ -2 ( $2.4 \text{ \AA}$ ). Thus, the portal size of  $C_1$  symmetrical cage  $C_1$ -1 allows the carbohydrate Oct- $\alpha$ -Glc to partially enter inside the cavity, what is not possible with the  $C_3$  symmetrical parent. The key role of the OH unit of the guest was further investigated using  $C_1$ -(+)-1 as host and an Oct- $\alpha$ -Glc derivative presenting four acetate protecting groups as guest. The binding constant was ten times lower with the protected carbohydrate than with the parent Oct- $\alpha$ -Glc compound, highlighting the importance of the alcohol functions of the guest in the complexation process (Figures S70 and S71). Thus, hosts  $C_1$ -1 and  $C_3$ -2 exhibit the same recognition units and cavity size, but  $C_1$ -1 is better preorganized to accommodate carbohydrates. Indeed, its binding motifs, are more easily accessible thanks to a wider window; hence much better binding constants are reached with  $C_1$ -1 than with  $C_3$ -2.

Another trend can be observed: the  $\alpha$  anomers of glucose and mannose are better recognized than the  $\beta$  ones with both the  $C_1$  and  $C_3$  symmetrical cages, the highest  $K_a$  values for the  $\alpha$  anomers being always obtained with the cage  $C_1$ -1. For instance,  $\alpha$ : $\beta$  diastereoselectivities of 100:1 and 10:1 are achieved with the  $C_1$ -(+)-1 hosts for glucose and mannose, respectively.  $C_1$ -(-)-1 and  $C_3$ -(-)-2 show even exclusive complexation of the  $\alpha$  anomer of glucose. In sharp contrast, when galactose is used as guest, the  $\beta$  anomer is much better complexed than the  $\alpha$  one, with both the  $C_1$  and  $C_3$  symmetrical cages (except with  $C_3$ -(-)-2 that displays no recognition properties toward the two anomers of this guest). Indeed, an exclusive diastereoselectivity is achieved with the  $C_1$ -(+)-1 and  $C_1$ -(-)-1 cages: the  $\beta$ -galactose is complexed with binding constant of  $1229 M^{-1}$  and  $2416 M^{-1}$  respectively, whereas no recognition



can be detected with  $\alpha$ -galactose. The  $C_3$ -(+)-2 cage displays a lower 1:3  $\alpha$ -galactose/ $\beta$ -galactose diastereoselectivity. A modest enantioselectivity is reached with both **1** and **2** when the glucose is used as a guest. With mannose as guest, an enantioselectivity of 3:1 is achieved with the  $C_1$  symmetrical cage  $C_1$ -1 whereas a ratio of 1.5:1 is achieved with the  $C_3$  symmetrical receptor  $C_3$ -2. The  $C_3$ -2 receptor exhibits remarkable enantioselectivity for galactose, since the  $C_3$ -(+)-2 cage gives binding constant of 249 and 677  $M^{-1}$  for  $\alpha$ -galactose and  $\beta$ -galactose, whereas its enantiomer  $C_3$ -(-)-2 is not able to complex these two guests. Finally, a striking substrate selectivity is also evidenced, in particular with the  $C_1$ -1 receptors. A  $K_a$  of 4656  $M^{-1}$  is measured for  $C_1$ -(+)-1 for  $\alpha$ -glucose whereas the  $\alpha$ -galactose is not recognized; similarly, the  $C_1$ -(-)-1 cage presents a  $K_a$  of 2416  $M^{-1}$  for  $\beta$ -galactose whereas no binding constant can be determined with  $\beta$ -glucose as a guest. Thus, these  $C_1$  symmetrical receptors can fully discriminate galactose from glucose, offering the way to complex exclusively one or the other. This is even more remarkable since these two carbohydrates have the same functional groups and almost the same size and differ only by the stereochemistry of a single stereogenic center.

## Conclusion

In conclusion, the use of HFIP allowed for the formation of the  $C_3$  symmetrical cage  $C_3$ -2, whereas the more "classical" condition using formic acid, provided the  $C_1$  hemicryptophane  $C_1$ -1. This highlights the significance of this former procedure that strongly affects the selectivity of the formation of the CTV units, when compared to previous methods. The  $C_1$  symmetrical receptor complexes carbohydrates much more efficiently than its  $C_3$  symmetrical counterpart. This is attributed to the presence of the larger window in the  $C_1$  symmetrical receptor, affording a direct access to the recognition sites of the receptor. In sharp contrast, the access to the cavity of the  $C_3$  symmetrical parent is hampered by small windows. High stereoselectivity was also reached with the dissymmetrical cage  $C_1$ -1, that was also found to discriminate galactose from glucose. Thus, the use of lowered symmetry cages could give rise to receptors with improved recognition properties, mimicking key features of biological systems.

## Experimental Section

**General information:** Commercial reagents were used directly as received without further purification. Dichloromethane was dried prior to use through standard procedures or obtained from a solvent drying system (MB-SPS-800).  $^1H$  and  $^{13}C$  NMR spectra were recorded on a Bruker AC 300, Bruker AC 400, Bruker 500 HD spectrometers. Chemical shifts are reported in ppm on the  $\delta$  scale relative to residual  $CDCl_3$  ( $\delta = 7.26$  for  $^1H$  NMR and  $\delta = 77.16$  for  $^{13}C$  NMR),  $CD_2Cl_2$  ( $\delta = 5.32$  for  $^1H$  NMR and  $53.84$  for  $^{13}C$  NMR) as the internal references. Coupling constants ( $J$ ) are reported in Hertz (Hz). Multiplicities are described with the standard following abbreviations: s=singlet, br=broad, d=doublet, t=triplet, q=quadruplet, m=multiplet. Column chromatography was performed

with gel 60 (Macherey-Nagel® Si 60, 0.040–0.063 mm). Analytical thin layer chromatography (TLCs) was carried out on Merck®Kieselgel 60 F254 plates and achieved under a 254 nm UV light. High-resolution mass spectra (HRMS) were performed on a SYNAPT G2 HDMS (Waters) spectrometer equipped with atmospheric pressure ionization source (API) pneumatically assisted.

**$C_1$ -symmetrical cage  $C_1$ -1:** Compound **7** (1 g, 0.98 mmol) was dissolved in formic acid (1 L). The mixture was stirred vigorously and heated at 50 °C for 1 day. Then the solvent was removed under vacuum. The residue was dissolved in  $CH_2Cl_2$  (50 mL) and was washed by 1 M NaOH solution (3 × 50 mL). The organic phase was dried over anhydrous  $Na_2SO_4$ , then concentrated in vacuum to give a yellow solid compound. The crude compound was purified on silica gel column chromatography using a mixture solution of  $CH_2Cl_2/MeOH$  (15:1) as eluent to give the pure **1** (294 mg, 42%). White solid. Tm : 157 °C.  $^1H$  NMR (300 MHz,  $CD_2Cl_2$ ):  $\delta$  7.55 (s, 1H), 7.13 (t,  $J = 4.1$  Hz, 1H), 7.03 (d,  $J = 8.5$  Hz, 1H), 6.90 (s, 1H), 6.87 (s, 1H), 6.83 (s, 1H), 6.71 (d,  $J = 8.4$  Hz, 1H), 6.47 (t,  $J = 4.1$  Hz, 1H), 5.77 (t,  $J = 5.2$  Hz, 1H), 4.74 (dd,  $J = 16.7, 13.6$  Hz, 2H), 4.43 (d,  $J = 13.2$  Hz, 1H), 4.25–4.05 (m, 5H), 4.01–3.94 (m, 1H), 3.93 (s, 3H), 3.79 (s, 3H), 3.79 (s, 3H), 3.54 (dd,  $J = 4.52$  Hz, 19.2 Hz, 3H), 3.48–3.39 (m, 1H), 3.39–3.28 (m, 1H), 3.23–3.05 (m, 3H), 2.66 (d,  $J = 16.8$  Hz, 1H), 2.58 (d,  $J = 5.5$  Hz, 1H), 2.46 (d,  $J = 16.6$  Hz, 1H), 2.36 (d,  $J = 16.0$  Hz, 1H), 1.97–1.68 (m, 5H), 1.33–1.23 (m, 4H).  $^{13}C$  NMR (101 MHz,  $CD_2Cl_2$ ):  $\delta$  170.3, 170.1, 169.9, 150.9, 149.2, 148.9, 148.3, 146.4, 146.2, 134.3, 134.1, 133.9, 133.5, 132.9, 132.2, 125.0, 118.3, 117.6, 115.7, 115.2, 113.4, 68.5, 67.9, 67.6, 60.6, 58.7, 57.8, 57.3, 56.3, 56.1, 36.5, 36.4, 36.2, 35.9, 29.8, 29.1, 28.8, 28.4. IR  $cm^{-1}$ : 3622, 3395, 3283, 2920, 2830, 2449, 2260, 2184, 2069, 2031, 1659, 1654, 1517, 1483, 1442, 1377, 1263, 1205, 1149, 1133, 1083, 1005, 990, 964, 885, 738, 701, 620. HRMS (ESI):  $m/z$   $[M + H]^+$  calcd for  $C_{39}H_{48}N_4O_9$ , 717.3494; found at 717.3494.

**$C_3$ -symmetrical cage  $C_3$ -2:** Compound **7** (160 mg, 0.16 mmol, 1.0 equiv.) was dissolved into 160 mL of chloroform/HFIP (1/1). After complete dissolution of **7**,  $KHSO_4$  (21 mg, 0.15 mmol, 0.9 equiv.) was added. The reaction mixture was stirred for 20 h. The solvents were evaporated, and the resulting oil was dissolved in 20 mL of dichloromethane, washed with water (30 mL) and extracted with dichloromethane (2 × 30 mL). The combined organic layers were dried over  $Na_2SO_4$  and evaporated. The crude compound was purified on silica gel column by chromatography using a mixture solution of  $CH_2Cl_2/MeOH$  (15:1) as eluent to give the pure **2** (31 mg, 27%). Beige solid. Tm: 180–181 °C.  $^1H$  NMR (300 MHz,  $CD_2Cl_2$ ):  $\delta$  6.88 (s, 3H), 6.82 (s, 3H), 6.52 (t,  $J = 6.2$  Hz, 3H), 4.75 (d,  $J = 13.7$  Hz, 3H), 4.16 (dd,  $J = 4.8$  Hz, 6.3 Hz, 6H), 3.81 (s, 9H), 3.58–3.47 (m, 3H), 3.52 (d,  $J = 13.8$  Hz, 3H), 3.15–3.02 (m, 3H), 2.66 (d,  $J = 15.9$  Hz, 3H), 2.09 (d,  $J = 15.9$  Hz, 3H), 2.01–1.85 (m, 3H), 1.76–1.61 (m, 3H).  $^{13}C$  NMR (75 MHz,  $CD_2Cl_2$ ):  $\delta$  170.2, 149.1, 146.5, 133.4, 132.3, 117.5, 113.5, 68.1, 57.8, 56.1, 36.5, 36.3, 28.5. IR:  $cm^{-1}$  3467, 3305, 2921, 2850, 2411, 2355, 2260, 2069, 1658, 1603, 1536, 1441, 1376, 1265, 1205, 1182, 1046, 1023, 989, 968, 885, 737, 588, 534. HRMS (ESI):  $m/z$   $[M + H]^+$  calcd for  $C_{39}H_{48}N_4O_9$ , 717.3494; found at 717.3493.

**Separation of compounds  $C_1$ -1 and  $C_3$ -2 on chiral stationary phases:**  $C_1$ -symmetrical cage  $C_1$ -1,  $C_3$ -symmetrical cage  $C_3$ -2 and their enantiomers can be separated by chiral chromatography by using (*S,S*)-Whelk-O1 (250 × 10 mm) and Chiralpak IF (250 × 10 mm). (*M*)- $C_1$ :  $\alpha_D^{25} = +8.5$  ( $c = 0.18$ ,  $CH_2Cl_2$ ); (*P*)- $C_1$ :  $\alpha_D^{25} = -8.5$  ( $c = 0.15$ ,  $CH_2Cl_2$ ); (*M*)- $C_3$ :  $\alpha_D^{25} = +28$  ( $c = 0.2$ ,  $CH_2Cl_2$ ); (*P*)- $C_3$ :  $\alpha_D^{25} = -28$  ( $c = 0.24$ ,  $CH_2Cl_2$ ).

**Titration experiments:** A solution of host cage (1.0 mM in  $CD_2Cl_2$ , 500  $\mu L$ ) was titrated in NMR tubes with aliquots of a concentrated solution (10 mM in  $CD_2Cl_2$ ) of sugar. The chemical shifts of protons of the host were measured after each addition and plotted as a

function of the guest/host ratio ( $[G]/[H]$ ). The association constant  $K_g$  was obtained by nonlinear least-squares fitting of these plots using the Bindfit program.

- [1] a) D. Zhang, T. K. Ronson, Y.-Q. Zou, J. R. Nitschke, *Nat. Chem. Rev.* **2021**, *5*, 168–182; b) S. Pullen, J. Tessarolo, G. H. Clever, *Chem. Sci.* **2021**, *12*, 7269–7293; c) M. J. Hardie, *Chem. Lett.* **2016**, *45*, 1336–1346.
- [2] a) T. Brotin, J.-P. Dutasta, *Chem. Rev.* **2009**, *109*, 88–130; b) H. Xie, T. J. Finnegan, V. W. L. Gunawardana, R. Z. Pavlović, C. E. Moore, J. D. Badjić, *J. Am. Chem. Soc.* **2021**, *143*, 3874–3880; c) K. Hermann, Y. Ruan, A. M. Hardin, C. M. Hadad, J. D. Badjić, *Chem. Soc. Rev.* **2015**, *44*, 500–514; d) M. Mastalerz, *Acc. Chem. Res.* **2018**, *51*, 2411–2422.
- [3] K. Jie, Y. Zhou, E. Li, F. Huang, *Acc. Chem. Res.* **2018**, *51*, 2064–2072.
- [4] P. Howlader, E. Zangrando, P. S. Mukherjee, *J. Am. Chem. Soc.* **2020**, *142*, 9070–9078.
- [5] a) M. Yamashina, Y. Tanaka, R. Lavendomme, T. K. Ronson, M. Pittelkow, J. R. Nitschke, *Nature* **2019**, *574*, 511–515; b) I. A. Riddell, M. M. J. Smulders, J. K. Clegg, J. R. Nitschke, *Chem. Commun.* **2011**, *47*, 457–459; c) D. Zhang, T. K. Ronson, W. Wang, L. Xu, H.-B. Yang, J. R. Nitschke, *Angew. Chem. Int. Ed.* **2021**, *60*, 11789–11792; *Angew. Chem.* **2021**, *133*, 11895–11898; *Angew. Chem. Int. Ed.* **2021**, *60*, 11789–11792.
- [6] S. Akine, M. Miyashita, T. Nabeshima, *J. Am. Chem. Soc.* **2017**, *139*, 4631–4634.
- [7] a) P. A. Gale, J. T. Davis, J. T. R. Quesada, *Chem. Soc. Rev.* **2017**, *46*, 2497–2519; b) G. Zhang, M. Mastalerz, *Chem. Soc. Rev.* **2014**, *43*, 1934–1947.
- [8] D. Yang, J. Zhao, Y. Zhao, Y. Lei, L. Cao, X.-J. Yang, M. Davi, N. de Sousa Amadeu, C. Janiak, Z. Zhang, Y.-Y. Wang, B. Wu, *Angew. Chem. Int. Ed.* **2015**, *54*, 8658–8661; *Angew. Chem.* **2015**, *127*, 8782–8785.
- [9] M. Yoshizawa, J. K. Klosterman, M. Fujita, *Angew. Chem. Int. Ed.* **2009**, *48*, 3418–3438; *Angew. Chem.* **2009**, *121*, 3470–3490.
- [10] S. Zarra, D. M. Wood, D. A. Roberts, J. R. Nitschke, *Chem. Soc. Rev.* **2015**, *44*, 419–432.
- [11] a) C. J. Brown, F. D. Toste, R. G. Bergman, K. N. Raymond, *Chem. Rev.* **2015**, *115*, 3012–3035; b) M. Morimoto, S. M. Bierschenk, K. T. Xia, R. G. Bergman, K. N. Raymond, F. Dean Toste, *Nat. Catal.* **2020**, *3*, 969–984.
- [12] Q. Zhang, K. Tiefenbacher, *Nat. Chem.* **2015**, *7*, 197–202.
- [13] S. H. A. M. Leenders, R. Gramage-Doria, B. De Bruin, J. N. H. Reek, *Chem. Soc. Rev.* **2015**, *44*, 433–448.
- [14] C. Gaeta, P. La Manna, M. De Rosa, A. Soriente, C. Talotta, P. Neri, *ChemCatChem* **2021**, *13*, 1638–1658.
- [15] S. Roland, J. Meijide Suarez, M. Sollogoub, *Chem. Eur. J.* **2018**, *24*, 12464–12473.
- [16] D. Matt, J. Harrowfield, *ChemCatChem* **2021**, *13*, 153–168.
- [17] G. Olivo, G. Capocasa, D. Del Giudice, O. Lanzalunga, S. Di Stefano, *Chem. Soc. Rev.* **2021**, *50*, 7681–7724.
- [18] a) S. C. Bete, M. Otte, *Angew. Chem. Int. Ed.* **2021**, *60*, 18582–18586; *Angew. Chem.* **2021**, *133*, 18730–18734; b) M. Otte, M. Lutz, R. J. M. Klein Gebbink, *Eur. J. Org. Chem.* **2017**, 1657–1661.
- [19] a) C. T. McTernan, J. A. Davies, J. R. Nitschke, *Chem. Rev.* **2022**, in press, doi.org/10.1021/acs.chemrev.1c00763; b) J. P. Carpenter, C. T. McTernan, T. K. Ronson, J. R. Nitschke, *J. Am. Chem. Soc.* **2019**, *141*, 11409–11413; c) F. J. Rizzuto, J. P. Carpenter, J. R. Nitschke, *J. Am. Chem. Soc.* **2019**, *141*, 9087–9095; d) D. Zhang, T. K. Ronson, L. Xu, J. R. Nitschke, *J. Am. Chem. Soc.* **2020**, *142*, 9152–9157; e) F. J. Rizzuto, J. R. Nitschke, *Nat. Chem.* **2017**, *9*, 903–908.
- [20] a) Q.-F. Sun, S. Sato, M. Fujita, *Angew. Chem. Int. Ed.* **2014**, *53*, 13510–13513; *Angew. Chem.* **2014**, *126*, 13728–13731; b) D. Fujita, K. Suzuki, S. Sato, M. Yagi-Utsumi, Y. Yamaguchi, N. Mizuno, T. Kumasaka, M. Takata, M. Noda, S. Uchiyama, K. Kato, M. Fujita, *Nat. Commun.* **2012**, *3*, 1–7.
- [21] A. M. Johnson, R. J. Hooley, *Inorg. Chem.* **2011**, *50*, 4671–4673.
- [22] D. Preston, J. E. Barnsley, K. C. Gordon, J. D. Crowley, *J. Am. Chem. Soc.* **2016**, *138*, 10578–10585.
- [23] a) W. M. Bloch, J. J. Holstein, W. Hiller, G. H. Clever, *Angew. Chem. Int. Ed.* **2017**, *56*, 8285–8289; *Angew. Chem.* **2017**, *129*, 8399–8404; b) S. Sudan, R.-J. Li, S. M. Jansze, A. Platzek, R. Rudolf, G. H. Clever, F. Fadaei-Tirani, R. Scopelliti, K. Severin, *J. Am. Chem. Soc.* **2021**, *143*, 1773–1778; c) W. M. Bloch, Y. Abe, J. J. Holstein, C. M. Wandtke, B. Dittrich, G. H. Clever, *J. Am. Chem. Soc.* **2016**, *138*, 13750–13755; d) S. Pullen, J. Tessarolo, G. H. Clever, *Chem. Sci.* **2021**, *12*, 7269–7293.
- [24] T. K. Ronson, J. Fisher, L. P. Harding, P. J. Rizkallah, J. E. Warren, J. M. J. Hardie, *Nat. Chem.* **2009**, *1*, 212–216.
- [25] a) P. Ríos, T. J. Mooibroek, T. S. Carter, C. Williams, M. R. Wilson, M. P. Crump, A. P. Davis, *Chem. Sci.* **2017**, *8*, 4056–4061; b) R. A. Tromans, T. S. Carter, L. Chabanne, M. P. Crump, H. Li, J. V. Matlock, M. G. Orchard, A. P. Davis, *Nat. Chem.* **2019**, *11*, 52–56; c) R. A. Tromans, S. K. Samanta, A. M. Chapman, A. P. Davis, *Chem. Sci.* **2020**, *11*, 3223–3227; d) T. J. Mooibroek, M. P. Crump, A. P. Davis, *Org. Biomol. Chem.* **2016**, *14*, 1930–1933.
- [26] C. Li, A.-D. Manick, M. Jean, M. Albalat, N. Vanthuyne, J.-P. Dutasta, X. Bugaut, B. Chatelet, A. Martinez, *J. Org. Chem.* **2021**, *86*, 15055–15062.
- [27] O. Della-Negra, Y. Cirillo, T. Brotin, J.-P. Dutasta, P.-L. Saïdi, B. Chatelet, A. Martinez, *Chem. Commun.* **2022**, *58*, 3330–3333.
- [28] a) C. Andraud, C. Garcia, A. Collet, in *Circular Dichroism, Principles and Applications, S-Substituted Aromatics and Exciton Chirality*, (Ed. N. Berova, K. Nakanishi and R. W. Woody) Wiley-VCH, Weinheim, 2nd edn, **2000**; b) J. Canceill, A. Collet, J. Gabard, G. Gottarelli, G. P. Spada, *J. Am. Chem. Soc.* **1985**, *107*, 1299–1308; c) J. Canceill, A. Collet, G. Gottarelli, P. Palmieri, *J. Am. Chem. Soc.* **1987**, *109*, 6454–6464.
- [29] T. Angata, A. Varki, *Chem. Rev.* **2002**, *102*, 439–469.
- [30] R. Kannagi, in *Carbohydrate-based drug discovery*, (Ed. C.-H. Wong), Wiley-VCH, Weinheim, Germany **2003**, Ch 30.
- [31] a) P. Davis, *Chem. Soc. Rev.* **2020**, *49*, 2531–2545; b) M. Mazik, *Chem. Soc. Rev.* **2009**, *38*, 935–956; c) T. J. Mooibroek, J. M. Casas-Solvas, R. L. Harniman, C. M. Renney, T. S. Carter, M. P. Crump, A. P. Davis, *Nat. Chem.* **2015**, *8*, 69–74.
- [32] a) O. Francesconi, S. Roelens, *ChemBioChem* **2019**, *20*, 1329–1346; b) M. Mazik, H. Cava, *J. Org. Chem.* **2006**, *71*, 2957–2963; c) M. Stapf, W. Seichter, M. Mazik, *Eur. J. Org. Chem.* **2020**, *2020*, 4900–4915; d) S. Kaiser, C. Geffert, M. Mazik, *Eur. J. Org. Chem.* **2019**, *2019*, 7555–7562; e) O. Francesconi, F. Milanese, C. Nativi, S. Roelens, *Angew. Chem. Int. Ed.* **2021**, *60*, 11168–11172; *Angew. Chem.* **2021**, *133*, 11268–11272; f) T. S. Carter, T. J. Mooibroek, P. F. N. Stewart, M. P. Crump, M. C. Galan, A. P. Davis, *Angew. Chem. Int. Ed.* **2016**, *55*, 9311–9315; *Angew. Chem.* **2016**, *128*, 9457–9461.
- [33] a) S. Anderson, U. Neidlein, V. Gramlich, F. Diederich, *Angew. Chem. Int. Ed.* **1995**, *34*, 1596–1600; *Angew. Chem.* **1995**, *107*, 1722–1725; b) Y. Jang, R. Natarajan, Y. H. Ko, K. Kim, *Angew. Chem. Int. Ed.* **2014**, *53*, 1003–1007; *Angew. Chem.* **2014**, *53*, 1021–1025; c) O. Francesconi, M. Martinucci, L. Badii, C. Nativi, S. Roelens, *Chem. Eur. J.* **2018**, *24*, 6828–6836; d) P. K. Mandal, B. Kauffmann, H. Destecroix, Y. Ferrand, A. P. Davis, I. Huc, *Chem. Commun.* **2016**, *52*, 9355–9358; e) F. Amrhein, J. Lippe, M. Mazik, *Org. Biomol. Chem.* **2016**, *14*, 10648–10659; f) O. Francesconi, F. Milanese, C. Nativi, S. Roelens, *Chem. Eur. J.* **2021**, *27*, 10456–10460.
- [34] a) C. Ke, H. Destecroix, M. P. Crump, A. P. Davis, *Nat. Chem.* **2012**, *4*, 718–723; b) T. J. Mooibroek, J. M. Casas-Solvas, R. L. Harniman, C. M. Renney, T. S. Carter, M. P. Crump, A. P. Davis, *Nat. Chem.* **2016**, *8*, 69–74; c) Y. Ferrand, M. P. Crump, A. P. Davis, *Science* **2007**, *318*, 619–622; d) A. Long, O. Perraud, M. Albalat, V. Robert, J.-P. Dutasta, A. Martinez, *J. Org. Chem.* **2018**, *83*, 6301–6306; e) O. Perraud, A. Martinez, J.-P. Dutasta, *Chem. Commun.* **2011**, *47*, 5861–5863; f) O. Francesconi, A. Ienco, G. Moneti, C. Nativi, S. Roelens, *Angew. Chem. Int. Ed.* **2006**, *45*, 6693–6696; *Angew. Chem.* **2006**, *118*, 6845–6848; g) F. Amrhein, M. Mazik, *Eur. J. Org. Chem.* **2021**, *2021*, 6282–6303.
- [35] a) D. Yang, L. K. S. von Krbek, L. Yu, T. K. Ronson, J. D. Thoburn, J. P. Carpenter, J. L. Greenfield, D. J. Howe, B. Wu, J. R. Nitschke, *Angew. Chem. Int. Ed.* **2021**, *60*, 4485–4490; *Angew. Chem.* **2021**, *133*, 4535–4540; b) B. J. J. Timmer, A. Kooijman, X. Schaapkens, T. J. Mooibroek,

- Angew. Chem. Int. Ed.* **2021**, *60*, 16178–16183; *Angew. Chem.* **2021**, *133*, 16314–16319; c) X. Schaapkens, R. N. Van Sluis, E. O. Bobylev, J. N. H. Reek, T. J. Mooibroek, *Chem. Eur. J.* **2021**, *27*, 13719–13724.
- [36] a) N. Chandramouli, Y. Ferrand, G. Lautrette, B. Kauffmann, C. D. Mackereth, M. Laguerre, D. Dubreuil, I. Huc, *Nat. Chem.* **2015**, *7*, 334–341; b) S. Pramanik, B. Kauffmann, S. Hecht, Y. Ferrand, I. Huc, *Chem. Commun.* **2021**, *57*, 93–96; c) S. Saha, B. Kauffmann, Y. Ferrand, I. Huc, *Angew. Chem. Int. Ed.* **2018**, *57*, 13542–13546; *Angew. Chem.* **2018**, *130*, 13730–13734; d) P. Mateus, B. Wicher, Y. Ferrand, I. Huc, *Chem. Commun.* **2018**, *54*, 5078–5081; e) P. Mateus, N. Chandramouli, C. D. Mackereth, B. Kauffmann, Y. Ferrand, I. Huc, *Angew. Chem. Int. Ed.* **2020**, *59*, 5797–5805; *Angew. Chem.* **2020**, *132*, 5846–5854.
- [37] D. B. Hibbert, P. Thordarson, *Chem. Commun.* **2016**, *52*, 12792–12805; URL: <http://app.supramolecular.org/bindfit/>.
- [38] a) J. B. Maglic, R. Lavendomme, MoloVol: an Easy-to-Use Program to Calculate Various Volumes and Surface Areas of Chemical Structures and Identify Cavities, *ChemRxiv.*, September 20, **2021**, ver. 1 DOI: 10.26434/chemrxiv-2021-dss1j; b) E. F. Pettersen, T. D. Goddard, C. C. Huang, G. S. Couch, D. M. Greenblatt, E. C. Meng, T. E. Ferrin, *J. Comput. Chem.* **2004**, *25*, 1605–1612.
- [39] a) D. Zhang, A. Martinez, J.-P. Dutasta, *Chem. Rev.* **2017**, *117*, 4900–4942; b) Y. Makita, N. Katayama, H.-H. Lee, T. Abe, K. Sogawa, A. Nomoto, S.-I. Fujiwara, A. Ogawa, *Tetrahedron Lett.* **2016**, *57*, 5112–5115.